CHEMISTRY
A EUROPEAN JOURNAL

DOI: 10.1002/chem.200800586

Reactivity of Ammonia Ligands of the Antitumor Agent Cisplatin: A Unique Dodecanuclear Pt_4,Pd_4,Ag_4 Platform for Four Cytosine Model Nucleobases

Gunnar Kampf, Pablo J. Sanz Miguel, Marta Morell Cerdà, Michael Willermann, Alexandra Schneider, and Bernhard Lippert*[a]

Dedicated to Professor Jan Reedijk on the occasion of his retirement

Abstract: The reaction of a potential mono(nucleobase) model adduct of cisplatin, *cis*-$[Pt(NH_3)_2(1\text{-MeC-}N3)(H_2O)]^{2+}$ (**6**; 1-MeC: 1-methylcytosine), with the electrophile $[Pd(en)(H_2O)_2]^{2+}$ (en: ethylenediamine) at pH $\approx$6 yields a kinetic product **X** which is likely to be a dinuclear Pt,Pd complex containing 1-MeC^--*N3*,*N4* and OH bridges, namely *cis*-$[Pt(NH_3)_2(1\text{-}MeC^-\text{-}N3,N4)(OH)Pd(en)]^{2+}$. Upon addition of excess Ag^+ ions, conversion takes place to form a thermodynamic product, which, according to ^1H NMR spectroscopy and X-ray crystallography, is dominated by a μ-NH_2 bridge between the Pt^{II} and Pd^{II} centers. X-ray crystallography reveals that the compound crystallizes out of solution as a dodecanuclear complex containing four Pt^{II}, four Pd^{II}, and four Ag^+ entities: $[\{Pt_2(1\text{-}MeC^-\text{-}N3,N4)_2(NH_3)_2(NH_2)_2(OH)Pd_2(en)_2Ag\}_2\{Ag(H_2O)\}_2](NO_3)_{10}\cdot 6H_2O$ (**10**) is composed of a roughly planar array of the 12 metal ions, in which the metal ions are interconnected by μ-NH_2 groups (between Pt and Pd centers), μ-OH groups (between pairs of Pt atoms), and metal–metal donor bonds (Pt→Ag, Pd→Ag). The four 1-methylcytosinato ligands, which are stacked pairwise, as well as the four NH_3 ligands and parts of the en rings, are approximately perpendicular to the metal plane. Two of the four Ag ions (Ag2, Ag2′) of **10** are labile in solution and show the expected behavior of Ag^+ ions in water, that is, they are readily precipitated as AgCl by Cl^- ions. The resulting pentanuclear complex $[Pt_2Pd_2Ag(1\text{-}MeC^-)_2(NH_2)_2(OH)(NH_3)_2(en)_2](NO_3)_4\cdot 7H_2O$ (**11**) largely maintains the structural features of one half of **10**. The other two Ag^+ ions (Ag1, Ag1′) of **10** are remarkably unreactive toward excess NaCl. In fact, the pentanuclear complex $[Pt_2Pd_2AgCl(1\text{-}MeC^-)_2(NH_2)_2(OH)(NH_3)_2(en)_2](NO_3)_3\cdot 4.5H_2O$ (**12**), obtained from **10** with excess NaCl, displays a Cl^- anion bound to the Ag center (2.459(3) Å) and is thus a rare case of a crystallized "AgCl molecule".

Keywords: bioinorganic chemistry · bridging ligands · heterometallic complexes · nucleobases · platinum

Introduction

A central dogma of the chemistry of the antitumor agent *cis*-$PtCl_2(NH_3)_2$ (cisplatin) and its amine analogues, as well as of their *trans* isomers, is that the am(m)ine ligands behave as inert ligands.[1] Only occasionally, for example, in cases of binding of ligands with a high *trans* effect to *cis*-$(NH_3)_2Pt^{II}$ species, has substitution of ammonia ligands been reported.[2] A while ago, we reported on another case of reactivity of NH_3 ligands, namely μ-amide formation upon reaction of $[Pd(en)(H_2O)_2]^{2+}$ (en: ethylenediamine) with the NH_3 ligands in *trans*-$[Pt(NH_3)_2(HL)]^{2+}$ (HL: pyrazole (Hpz) or 2-aminopyridine (Hampy)).[3] Formation of the resulting mixed $Pt^{II}(\mu\text{-}NH_2)Pd^{II}$ species, which takes place in water and under mild conditions, was proposed to occur in two steps, namely by an initial anchoring of the Pd^{II} species at

[a] Dr. G. Kampf, Dr. P. J. Sanz Miguel,[+] M. Morell Cerdà, Dr. M. Willermann, Dr. A. Schneider, Prof. Dr. B. Lippert
Fakultät Chemie
Technische Universität Dortmund
Otto-Hahn-Strasse 6, 44221 Dortmund (Germany)
Fax: (+49) 231-755-3797
E-mail: bernhard.lippert@tu-dortmund.de

[+] Current address:
Departamento de Química Inorgánica
Universidad Autónoma de Madrid
28049 Madrid (Spain)

Supporting information for this article is available on the WWW under http://dx.doi.org/10.1002/chem.200800586.

an endocyclic N atom (for example, the second N atom of pyrazolate) or an exocyclic N atom (for example, the lone electron pair of the amino group of 2-aminopyridine), followed by condensation between a Pd–OH moiety and an NH_3 ligand of the Pt center (Scheme 1).

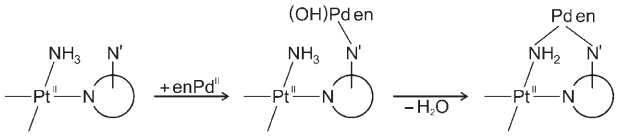

Scheme 1. Proposed two-step formation of the mixed $Pt^{II}(\mu\text{-}NH_2)Pd^{II}$ species.

In principle, analogous reactions should also be possible with *cis*-a_2Pt^{II} (a: NH_3 or amine) species replacing the $enPd^{II}$ species, but the kinetics are expected to be much slower.

The usual way to form homonuclear μ-NH_2 or μ-NHR complexes of the late transition metals involves aminolysis reactions of μ-OH species (Scheme 2), as demonstrated in

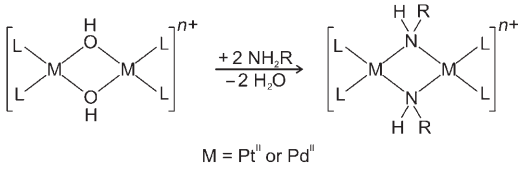

Scheme 2. Formation of homonuclear μ-NHR complexes by aminolysis of an μ-OH species.

numerous cases.[4] In these reactions, nucleophilic attack of the lone electron pair of the am(m)ine on the metal center initially takes place. μ-NH_2 complexes are likewise known with Pt^{IV} centers.[5] Their formation is facilitated by the remarkable acidification of NH_3 ligands when bound to Pt^{IV} species.

The aim of the present study was to extend our previous work[3] to Pt^{II} compounds containing the *cis* geometry and to include a model nucleobase, 1-methylcytosine (1-MeC), rather than other N-heterocyclic ligands, such as pyrazole or 2-aminopyridine. However, unlike 2-aminopyridine, the 1-methylcytosine nucleobase does not provide a lone electron pair at the exocyclic amino group.[6]

Results and Discussion

Reactions of $[Pd(en)(H_2O)_2]^{2+}$ with *cis*-$[Pt(NH_3)_2(py)(HL)]^{2+}$ (HL: Hpz (1) and Hampy (2); py: pyridine): Having previously demonstrated[3] that NH_3 and heterocyclic pyrazole or 2-aminopyridine ligands in *trans*-$[Pt(NH_3)_2(HL)_2]^{2+}$ can be bridged by $[Pd(en)]^{2+}$ with formation of mixed Pt,Pd complexes and μ-NH_2 or μ-L ligands, we were not surprised to see that **1** and **2** behaved analogously (Scheme 3). The ^{1}H NMR spectra of products **3** and **4** prepared in H_2O and dissolved in D_2O display the highly diagnostic μ-NH_2 resonance in the range of $\delta = 1.5$–1.6 ppm, and this signal undergoes a surprisingly slow exchange with

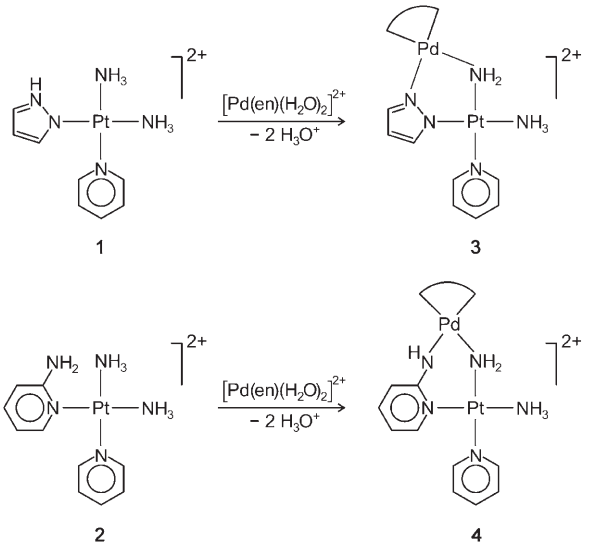

Scheme 3. Reactions of *cis*-$[Pt(NH_3)_2(py)(HPz)]^{2+}$ (**1**) and *cis*-$[Pt(NH_3)_2(py)(Hampy)]^{2+}$ (**2**) with $[Pd(en)(H_2O)_2]^{2+}$.

deuterium, as noted before.[3] The ^{1}H NMR spectrum of **3** and the ^{195}Pt-edited spectrum in D_2O at pD 7.2 are given in the Supporting Information. The ^{195}Pt–^{1}H coupling constants are in the expected range, and the relative intensities of the ^{1}H resonances are in agreement with expectations for a composition of $[Pt(\mu\text{-}pz)(\mu\text{-}NH_2)(NH_3)(py)Pd(en)]^{2+}$ (**3**). As in the case of the Pt,Pd complexes derived from *trans*-$[Pt(NH_3)_2L_2]^{2+}$, we propose that initial binding of $[Pd(en)]^{2+}$ occurs through an available N atom of L, which here would be the deprotonated pyrazole N2 position and the exocyclic amino group of the Hampy, respectively. The increase in Hpz acidity as a consequence of Pt^{II} coordination has been determined for **1** by applying pD-dependent ^{1}H NMR spectroscopy. The pK_a value of the Hpz ligand in **1** [Eq. (1)] was found to be 8.13 ± 0.05 (D_2O), which corresponds to 7.57 ± 0.05 in H_2O.

$$cis\text{-}[Pt(NH_3)_2(Hpz)(py)]^{2+} \rightleftharpoons cis\text{-}[Pt(NH_3)_2(pz)(py)]^{+} + H^{+} \quad (1)$$

As compared to free Hpz ($pK_a = 14.21$[7]), the acidity of the proton at the N atom thus increases by 6.6 log units in **1**. This feature clearly facilitates the initial Pd^{II} binding to the N2 atom of pz, which eventually leads to **3**.

In the case of the Hampy ligand in **2**, the available lone electron pair at the exocyclic amino group functions as an anchor for Pd^{II} coordination. Once the Pd^{II} species is bonded, the Hampy ligand undergoes rapid ionization to give the anionic ampy bridge.

Reactions of *cis*-[Pt(NH$_3$)$_2$(1-MeC-*N3*)(H$_2$O)]$^{2+}$: Treatment of *cis*-[PtCl(NH$_3$)$_2$(1-MeC-*N3*)]Cl·H$_2$O (**5**) with two equivalents of AgNO$_3$ in water yields *cis*-[Pt(NH$_3$)$_2$(1-MeC-*N3*)(H$_2$O)](NO$_3$)$_2$ (**6**) and *cis*-[Pt(NH$_3$)$_2$(1-MeC-*N3*)(OH)]NO$_3$ (**7**), depending on the pH value, both of which have been characterized by X-ray crystallography.[8] In solution, **6** and **7** exist in equilibrium with their dinuclear μ-OH condensation product *cis*-[(NH$_3$)$_2$Pt(1-MeC-*N3*)(OH)(1-MeC-*N3*)Pt(NH$_3$)$_2$]$^{3+}$ (**8**).[9] In a slow reaction, and in low yield, the dinuclear 1-methylcytosinato species *cis*-[(NH$_3$)$_2$Pt(1-MeC$^-$-*N3*,*N4*)$_2$Pt(NH$_3$)$_2$]$^{2+}$ (**9**) eventually forms; this product displays a head–tail arrangement of the two nucleobases.[10] Depending on conditions, oligomeric and intensely colored products, which presumably display similar (1-MeC$^-$-*N3*,*N4*) bridging modes of the nucleobases, are also formed with time.[11] A summary of the solution behavior of **6** is provided in Scheme 4, and the ^{1}H NMR spectroscopic chemical shifts are listed in Table 1.

In the presence of [Pd(en)(H$_2$O)$_2$]$^{2+}$ and its partially deprotonated form [Pd(OH)(en)(H$_2$O)]$^+$ (pD value in D$_2$O adjusted to 6 ± 0.5 by means of NaOD), two major products are formed according to ^{1}H NMR spectroscopy (Figure 1). Formation of an unknown species **X** is rapid, whereas the second major species, which develops more slowly but virtu-

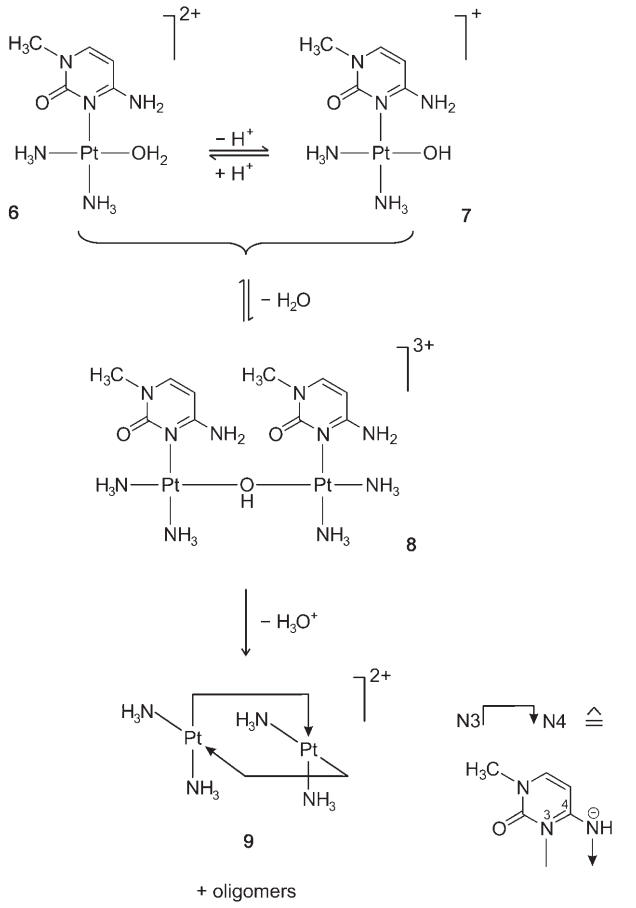

Scheme 4. Solution behavior of *cis*-[Pt(NH$_3$)$_2$(1-MeC-*N3*)(H$_2$O)](NO$_3$)$_2$ (**6**).

Table 1. ^{1}H NMR spectroscopic chemical shifts (δ [ppm], in D$_2$O) of the 1-methylcytosine complexes.

	H6[a]	H5[a]	CH$_3$[b]	CH$_2$(en)[c]	μ-NH$_2$[c]	pD
5	7.58	6.01	3.42	–	–	6.65
6/7	7.63	6.03	3.44	–	–	5.00
9	6.86	5.72	3.27	–	–	6.90
X	7.03	5.77	3.26	2.72	–	6.40
Y[d]	7.35	6.08	3.35	2.72	–	6.40
10	7.22	6.00	3.30	2.79 (s)	1.78 (brs)	6.08
					1.54 (brs)	
11	7.22	6.00	3.30	2.79 (s)	1.75 (brs)	6.60
					1.47 (brs)	
12	7.20	5.94	3.27	2.88 (m)	1.78 (brs)	8.20
	7.20	5.94	3.27	2.78 (m)	1.54 (brs)	3.70

[a] Doublets in all cases, with $^3J \approx 7.4$ Hz. [b] Singlets. [c] Abbreviations: s: singlet, m: multiplet, br: broad. [d] Addition of larger amounts of Ag$^+$ ions caused further shifts of cytosine resonances, for example, $\delta = 7.39$, 6.12, 3.36 ppm with 4 equivalents per atom of Pt.

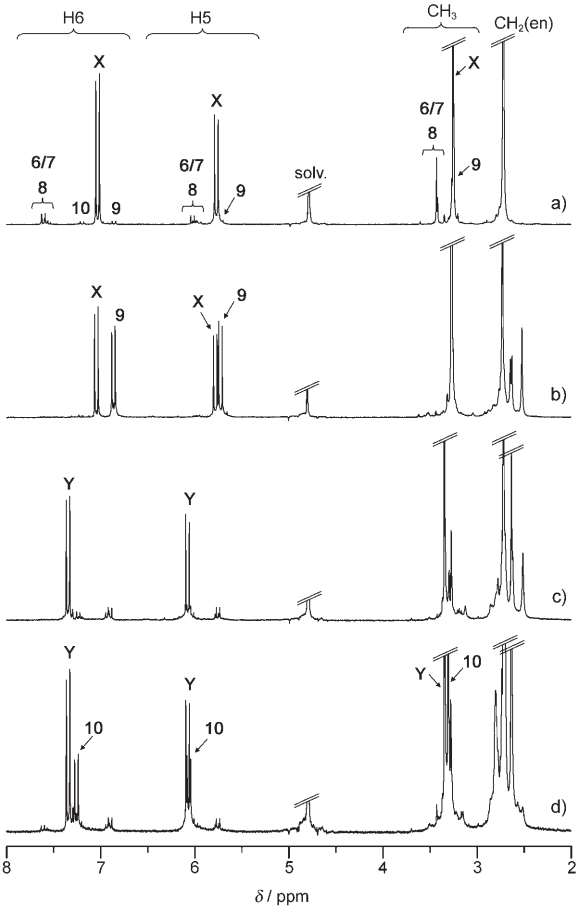

Figure 1. a) ^{1}H NMR spectrum of a reaction mixture of *cis*-[Pt(NH$_3$)$_2$(1-MeC-*N3*)(D$_2$O)]$^{2+}$ and [Pd(en)(D$_2$O)$_2$]$^{2+}$ with the pD value adjusted to 6.04, 6 h after mixing the respective Cl species, *cis*-[Pt(NH$_3$)$_2$(1-MeC-*N3*)Cl]Cl, and PdCl$_2$(en) with AgNO$_3$ (4 equiv) and centrifuging off AgCl. [Pt] = [Pd] = 0.05 M. b) ^{1}H NMR spectrum of the same mixture after 6 d at 22 °C. Note that resonances due to enPd–aqua/hydroxo species ($\delta = 2.5$–2.6 ppm) have formed. c) ^{1}H NMR spectrum after 6 d at 22 °C and addition of solid AgNO$_3$ (2 equiv per atom of Pt). Precipitation of **9** has occurred. d) ^{1}H NMR spectrum 5 d after addition of excess AgNO$_3$ with the sample kept at 22 °C.

ally without any side products, is assigned to the head–tail species **9** on the basis of its chemical shifts. As **9** is formed at the expense of **X**, new CH_2 resonances of the enPd^{II} species appear, upfield from those of **X**, which are probably due to $[Pd(en)(D_2O)_2]^{2+}$ and $[Pd(en)(OD)]_n^{n+}$ ($n=2$, 3, 4).[12] We tentatively assign **X** to a mixed Pt,Pd compound with the Pd^{II} center bonded to the deprotonated exocyclic N4-position of the cytosine nucleobase and bridged to the Pt^{II} atom by a hydroxo ligand (Scheme 5) for the following reasons: First, the stoichiometry between the 1-MeC$^-$ ligand and en in **X** is 1:1, according to ^{1}H NMR spectroscopic integrals. Second, freeze drying of a sample of **X**, obtained from *cis*-$[Pt(NH_3)_2(1\text{-MeC-}N3)(H_2O)]^{2+}$ (**6**) and $[Pd(en)(H_2O)_2]^{2+}$ at pH≈6 in H_2O a few hours after mixing of the components, with virtually no **9** formed yet, yields a product that in its ^{1}H NMR spectrum (in D_2O) does not display the resonances characteristic of μ-NH_2 bridge formation (see above and below). Third, the ^{195}Pt NMR spectroscopic chemical shift of **X** ($\delta=-1933$ ppm) is consistent with an N_3O environment for the Pt^{II} center, rather than an N_4 environment.[13] Fourth, the chemical shifts of the cytosine resonances in **X**, which are upfield (by approximately $\delta=0.6$ ppm for H6, $\delta=0.2$ ppm for H5, and $\delta=0.2$ ppm for CH_3) from those of **6** and **8**, are likewise indicative of metal binding to the anionic cytosine nucleobase through the N3 and N4 positions.[14]

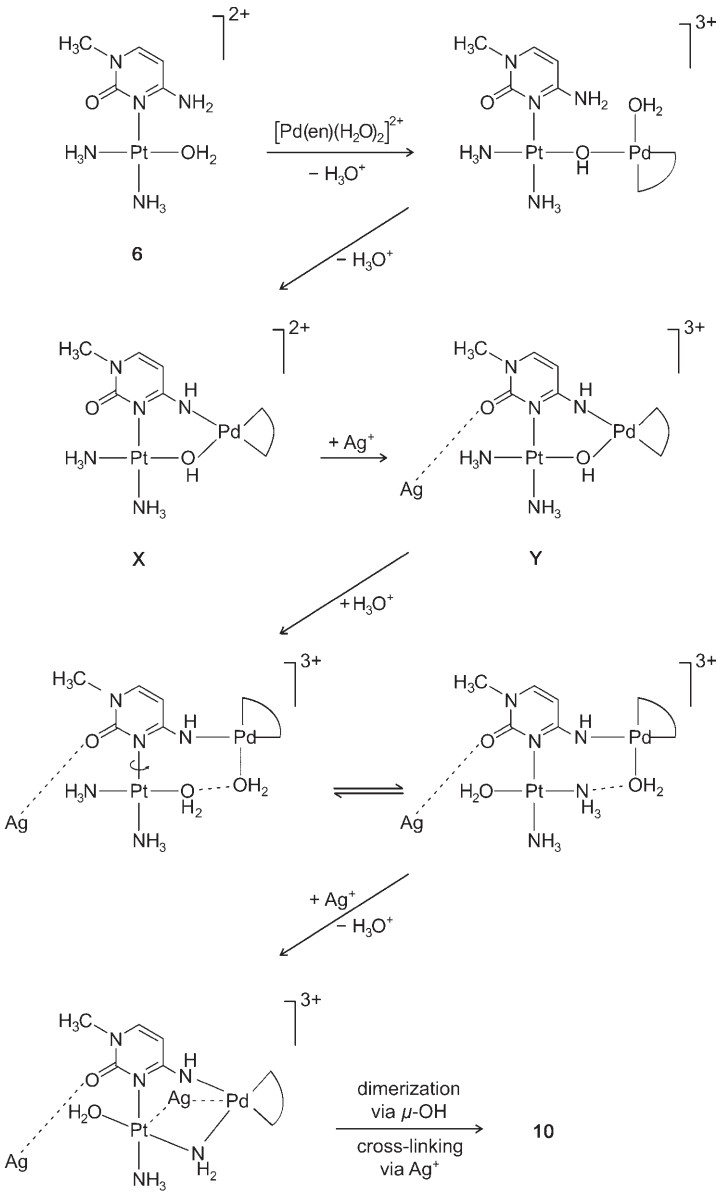

Scheme 5. Proposed scheme for the formation of **X**, **Y**, and **10**.

According to this proposal, the initial anchoring site of the Pd^{II} species is the aqua ligand of the Pt complex **6** rather than the heterocyclic nucleobase. As the exocyclic amino group of 1-MeC does not provide a lone electron pair for metal binding, as in the case of 2-aminopyridine or pyrazolate ligands (see Scheme 1 and reference [3]), Pd^{II} coordination to this site is not possible unless it has lost a proton. As an alternative, the Pd^{II} atom could anchor at the O2 site of 1-MeC, but the only way to form intermediate **X** would still be the subsequent (or simultaneous) formation of the Pt(μ-OH)Pd bond, followed by a reopening of the Pd–O2 bond, rotation of the 1-MeC moiety about the Pt–N3 bond, and Pd binding to the N4-position. We consider this way from **6** to **X** to be only a variant of that proposed in Scheme 5.

Remarkable ^{1}H NMR spectroscopic changes take place when solid $AgNO_3$ (two equivalents per Pt atom) is added to an aged solution containing essentially only **X** and **9** (Figure 1, spectrum c). The resonances of **9** virtually disappear as a consequence of precipitation. The resonances of **X** shift downfield at once, which is indicative of the formation of a new species, **Y**. In addition, there are a number of weak resonances due to the presence of cytosine compounds, one of which (with H6 at $\delta=7.26$ ppm, H5 at $\delta=6.00$ ppm, and CH_3 at $\delta=3.30$ ppm) has the second most intensive set of signals besides **Y** within 24 h at room temperature. The signals for the latter slowly grow in intensity over several days. As the shifts of these new resonances are identical to those of the structurally characterized $Pt_4Pd_4Ag_4$ complex **10** (see below), they are assigned to this species.

If, in a modification of the procedure described above, *cis*-$[Pt(NH_3)_2(1\text{-MeC-}N3)(D_2O)]^{2+}$ (**6**) and $[Pd(en)(D_2O)_2]^{2+}$ are mixed (1:1) and extra $AgNO_3$ (2 equiv per Pt) is added from the beginning, with the pD value adjusted to 6.4, the major species present at the beginning is species **Y**. Within 2–3 days at room temperature, the resonances due to compound **10** grow to be the second most abundant. Within 11 days, yellow cubes of **10** crystallize from solution. The identity of these crystals, obtained on a preparative scale, was established by X-ray analysis. Surprisingly, formation of the head–tail dimer **9** is negligible under these conditions (excess Ag^+ ions from the beginning; see the Supporting Information).

Before describing the structure of compound **10** in more detail, the nature of compound **Y** deserves some comment. The rapid conversion of **X** into **Y** by simple addition of Ag^+ ions suggests that **Y** is an Ag^+ adduct of **X** and, hence, that it represents a heteronuclear Pt,Pd,Ag compound, with the

Ag^+ center being bonded to either the O2 atom of 1-MeC$^-$ or being bonded by the Pt^{II} and Pd^{II} centers in a donor→acceptor interaction. The relatively large effect of the Ag^+ ions on the 1-methylcytosinato resonances seems to favor the first alternative, that is, binding to the O2 atom (Scheme 5). In fact, Ag^+ ion binding to the O2 position of N3,N4-metalated cytosine nucleobases has been observed before,[14,15] and the reversal of the chemical-shift changes upon addition of Cl^- ions to a solution of **10** (see below) further supports this view.

Formation of the Pt_4,Pd_4,Ag_4 complex 10: Both the ^{1}H NMR spectra and the results of the preparative work are consistent with the view that formation of the μ-NH_2 bridges seen in **10** requires "extra" Ag^+ ions. However, the way from Pt,Pd,Ag species **Y** to Pt_4,Pd_4,Ag_4 species **10** is not clear at present. According to the proposal made in Scheme 5, a central step in the formation of **10** from intermediate **X** and its Ag^+ adduct **Y** is the opening of the μ-OH bridge and a rotation of the Pt entity about the Pt–N3 (cytosine) bond. This is a prerequisite in order to accomplish the μ-NH_2 bridging seen in **10**.

X-ray crystal structure of [{Pt_2(1-MeC$^-$-*N3*,*N4*)$_2$(NH_3)$_2$-(NH_2)$_2$(OH)Pd_2(en)$_2$Ag}$_2${Ag(H_2O)}$_2$](NO_3)$_{10}$·6H_2O (10): As described above and reported in the Experimental Section, **10** is isolated upon reaction of *cis*-[Pt(NH_3)$_2$(1-MeC-*N3*)(H_2O)](NO_3)$_2$ (**6**) and [Pd(en)(H_2O)$_2$](NO_3)$_2$ in a 1:1 ratio at pH 6±0.5 in the presence of excess $AgNO_3$. Figure 2 gives different views of the cation of **10** or sections thereof, and Table 2 lists selected interatomic distances and angles. The cation is of C_2 symmetry and consists of a roughly planar array of 12 metal ions, namely 4 Pt^{II}, 4 Pd^{II}, and 4 Ag^+ ions. The 12 metal ions cover an area of approximately 11.2× 5.8 Å^2. The metals are interconnected by both in-plane ligands (μ-OH between pairs of Pt ions; μ-NH_2 between Pt1 and Pd1 and between Pt2 and Pd2, as well as the symmetry-related atoms) and by four out-of-plane bridging 1-methylcytosinato nucleobases. Each nucleobase forms two strong coordination bonds, to Pt at N3a,b (2.049(7), 2.032(7) Å) and to Pd at N4a,b (2.017(8)–2.039(7) Å), as well as two weak bonds, to Ag2 at O2a,b (2.572(6) Å; 2.508(6) Å)[16] and to Ag1 at N4a,b (2.743(8) Å; 2.388(8) Å). Thus, the 1-MeC$^-$ moiety can be regarded as a tetradentate ligand in **10**, with the deprotonated exocyclic N4 site acting as a bridging donor atom (Figure 3a).

While Pt–N and Pd–N bond lengths agree with expectations,[14] both the Ag–O and Ag–N lengths are significantly longer than in a mixed Pt,Ag complex of 1,5-dimethylcytosine,[15] in which they amount to 2.259(8) and 2.16(1) Å (average), respectively. The binding of the Ag1 and Ag1′ atoms is special in that all four of the surrounding d^8 metal ions, that is, Pd1, Pt1, Pt2, and Pd2 (for the case of Ag1), appear to be involved in weak donor→acceptor bond formation with the Ag^+ ion, based on geometrical considerations (intermetallic distances; positioning of the Ag1 atom relative to the filled d_{z^2} orbitals of the d^8 metal ions). The

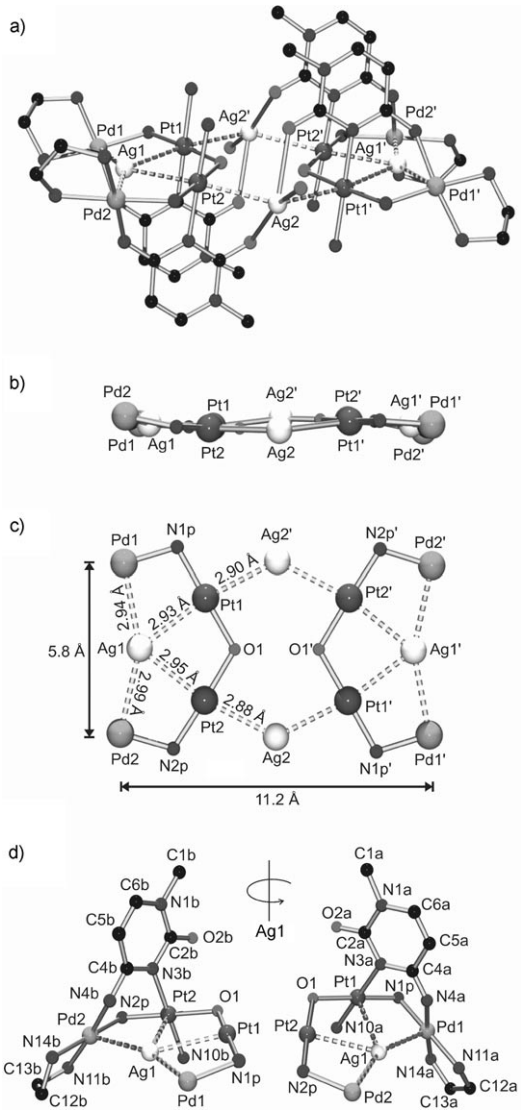

Figure 2. a) View of dodecanuclear cation **10**. b) Side view of the 12 metal ions. c) Top view of the 12 metal ions and the μ-NH_2 and μ-OH groups, together with intermetallic distances. For exact distances, see Table 2. d) Details of the Ag1 coordination geometry.

unreactivity of the Ag1 atom toward chloride ions (see below) is consistent with a special bonding situation. The distances between the Ag1 atom and the four d^8 metal ions (Pt1: 2.9284(12), Pt2: 2.9449(10), Pd1: 2.9422(12), Pd2: 2.9870(11) Å) are longer than those in typical donor–acceptor bonds between such metals,[12b,17,18] yet the number (four) of such interactions is larger in the present case. Altogether, and including the semichelating nitrate anion, the Ag1 atom is surrounded by eight atoms (Figure 3b).

The coordination geometry of the Ag2 atom is best described as a distorted trigonal bipyramid with three Ag–O bonds in the plane (two Ag–O2a,b cytosine bonds, one Ag–O2L bond to a water molecule) and two long axial contacts with Pt1′ (2.9028(13) Å) and Pt2 (2.8784(11) Å). These distances are in the range seen in related Pt,Ag complexes with

Table 2. Selected interatomic distances [Å] and angles [°] in **10**, **11**, and **12**.

	10	**11**	**12**
Ag1–Pt1	2.9284(12)	2.8269(10)	2.9120(11)
Ag1–Pt2	2.9449(10)	2.9301(17)	2.9652(11)
Ag1–Pd1	2.9422(12)	3.218(2)	3.0584(14)
Ag1–Pd2	2.9870(11)	2.9301(17)	2.9661(13)
Ag1–N4a	2.743(8)	3.076(16)	3.667(10)
Ag1–N4b	2.388(8)	2.403(10)	2.365(8)
Ag1–L	2.503(9)/2.593(11)[a]	2.503(9)[b]	2.459(3)[c]
Ag2–O2L	2.407(6)	–	–
Ag2–O2a	2.572(6)	–	–
Ag2–O2b	2.508(6)	–	–
Ag2–Pt1	2.9028(13)	–	–
Ag2–Pt2	2.8784(11)	–	–
Pt1–N1p	2.012(7)	2.016(8)	1.963(8)
Pt1–N3a	2.049(7)	2.034(9)	2.029(8)
Pt1–O1	2.046(5)	2.046(6)	2.033(7)
Pt1–Pd1	3.1734(13)	3.218(2)	3.1645(11)
Pt2–N2p	1.995(7)	1.998(7)	1.990(8)
Pt2–N3b	2.032(7)	2.035(8)	2.016(8)
Pt2–O1	2.063(5)	2.049(6)	2.054(6)
Pt2–Pd2	3.2432(14)	3.1782(12)	3.1558(11)
Pd1–N1p	2.000(7)	2.007(8)	1.999(8)
Pd1–N4a	2.017(8)	2.028(9)	1.995(9)
Pd2–N2p	2.002(8)	2.005(7)	2.004(8)
Pd2–N4b	2.039(7)	2.062(8)	2.088(9)

[a] Distance to the O41/O42 atoms of the nitrate group for **10**. [b] Distance to the O11 atom of the nitrate group for **11**. [c] Distance to the Cl1 atom for **12**.

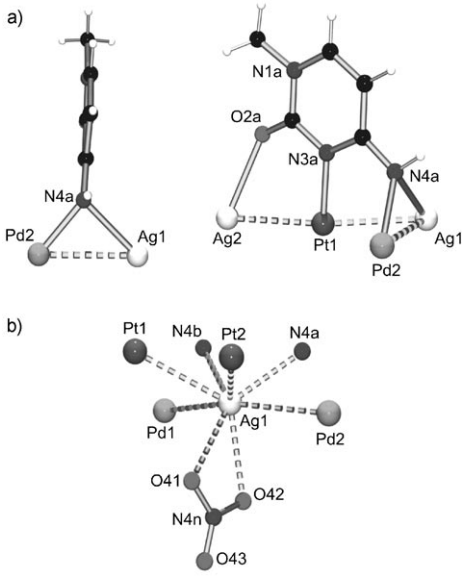

Figure 3. Structural details of **10**: a) Tetradentate nature of the 1-methylcytosinato ligand. b) Complete environment of the Ag1 center.

cytosinato and uracilato ligands.[15,19] Again, it could indicate weak donor→acceptor interactions between the Pt ions and the Ag^+ ion. Essentially, it would imply that all 4 Pt ions in **10** have undergone an extension of their coordination spheres from 4 to 4+2.

If the silver ions in **10** are ignored, the cation consists of two open Pd_2,Pt_2 half cycles, held together by two cytosinato bridges, two amido bridges, and a hydroxo bridge (Figure 4a).

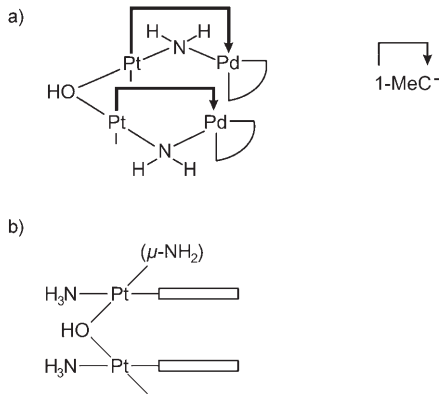

Figure 4. General structure of cation **10** (without the silver ions).

This pattern extends the previously reported ones in (frequently) dinuclear μ-amido and/or μ-hydroxo complexes containing two[4,20] or even three[21] different bridges. With regard to Pt and/or Pd representatives, the bonds between the metal ions and the NH_2 and OH ligands, respectively, are normal.[20] It is evident that the Ag2 and Ag2′ atoms are instrumental in keeping together the two halves of the molecular cation in the solid state. Furthermore, the relatively short separation of the two μ-OH sites (O1···O1′, 3.062 (11) Å) suggests that there are two weak hydrogen bonds between the protons of the OH groups and the neighboring oxygen atoms. Furthermore, there are four intramolecular hydrogen bonds (2.813(10) and 3.029(9) Å) between the cytosine O2 sites and the NH_3 ligands of the Pt centers.

The two cytosinato ligands in each half of the cation are parallel and stacked (3.49 Å). This feature (Figure 4b) probably also stabilizes the OH bridge. At the same time, this structural detail lends support to the idea that dinuclear Pt^{II}–nucleobase complexes containing a single OH bridge are feasible (see compound **8**), possibly even in DNA, as previously discussed.[22]

The packing motif of **10** is a repetition of the dodecanuclear Pt_4,Pd_4,Ag_4 platforms along the *c* axis to form ribbons (Figure 5). The cations are interconnected through pairs of hydrogen bonds between the water molecule (O2L) bonded to the Ag2 atom and an amino group of an en ligand (N11, $-x$, y, $0.5-z$) of a neighboring cation. The N···O distances are 2.987(10) Å. There are no additional intercationic hydrogen bonds, as the nitrate anions and water molecules effectively isolate the cations by forming multiple hydrogen bonds with the latter.

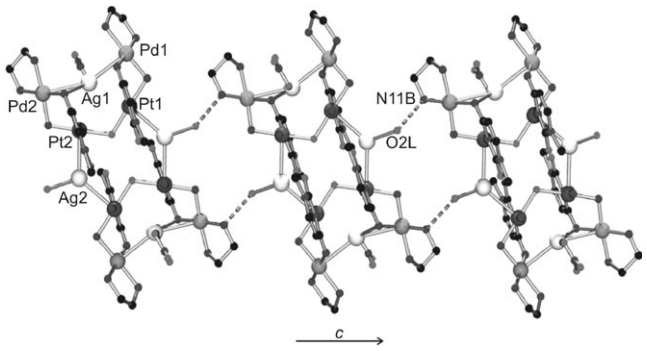

Figure 5. Packing of the cations of **10** with aqua ligands, O2L, accepting hydrogen bonds from the amino groups of the en ligands.

Solution behavior of 10: Figure 6a shows the ^{1}H NMR spectrum of **10** in D_2O. Chemical shifts of individual resonances are listed in Table 1. As mentioned above, the characteristic

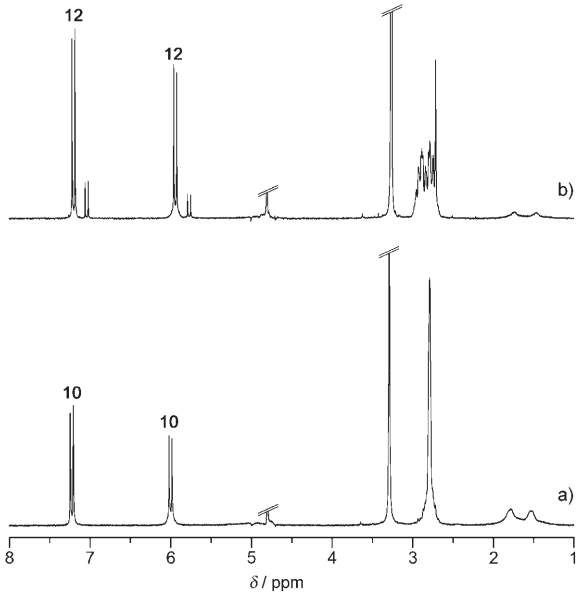

Figure 6. ^{1}H NMR spectra (D_2O) of a) isolated **10** (pD 6.1) and b) compound **12**, obtained upon addition of NaCl (4 equiv per molecule of **10**), centrifugation of AgCl, and acidification (DNO_3, pD 3.7). The minor components seen upon addition of acid are possibly due to compound **X**. The chemical shifts of **10** are virtually identical to those of **11** (compare with Table 1), which suggests that **10** is largely dissociated in solution according to the equation **10**⇌2 (**11**)+2 $AgNO_3$.

μ-NH_2 protons are observed as broad singlets at high field ($\delta = 1.78$ and 1.54 ppm). Unlike in the spectrum of **3** (see the Supporting Information, compare with above), ^{195}Pt satellites are not resolved. We propose that the spectrum corresponds essentially to a pentanuclear Pt_2,Pd_2,Ag species **11**, which represents a dissociation product of **10**, in which the O2-bonded Ag2 and Ag2′ ions are lost [Eq. (2)].

$$[Pt_4Pd_4Ag_4(1\text{-}MeC^-)_4(NH_2)_4(OH)_2(NH_3)_4(en)_4(H_2O)_2](NO_3)_{10}\ (\mathbf{10}) \rightleftharpoons 2\,[Pt_2Pd_2Ag(1\text{-}MeC^-)_2(NH_2)_2(OH)(NH_3)_2(en)_2](NO_3)_4\ (\mathbf{11}) + 2\,Ag^+ + 2\,NO_3^- + 2\,H_2O \quad (2)$$

This view is based on the observation that addition of two equivalents of NaCl per molecule of **10** in water leads to immediate precipitation of AgCl and crystallization of **11** (see below). The ^{1}H NMR spectrum does not change following the precipitation of AgCl and thereby confirms the formation of **11** upon dissolution of **10**.

Interestingly, addition of four equivalents of NaCl per molecule of **10** likewise leads to AgCl precipitation, yet an ^{1}H NMR spectrum is obtained that is significantly different from those of **10**/**11** (Figure 6b and Table 1). The newly formed compound **12**, which eventually crystallizes from the solution following filtration of AgCl, is again a pentanuclear Pt_2,Pd_2,Ag compound and is structurally similar to **11**, yet it contains a Cl^- ligand bonded to the Ag^+ ion. The formation of **12** can thus be described according to Equation (3).

$$[Pt_4Pd_4Ag_4(1\text{-}MeC^-)_4(NH_2)_4(OH)_2(NH_3)_4(en)_4(H_2O)_2](NO_3)_{10}\ (\mathbf{10}) + 4\,NaCl \rightleftharpoons 2\,[Pt_2Pd_2AgCl(1\text{-}MeC^-)_2(NH_2)_2(OH)(NH_3)_2(en)_2](NO_3)_3\ (\mathbf{12}) + 2\,AgCl\downarrow + 4\,NaNO_3 + 2\,H_2O \quad (3)$$

Apart from differences in the chemical shifts of the 1-MeC$^-$ and μ-NH_2 resonances in **10**/**11** and **12**, the appearance of the methylene protons of the en ligand is markedly different. In **12**, they appear as two multiplets (1:1 ratio) at $\delta \approx 2.88$ and 2.78 ppm. A feasible explanation, based on the X-ray crystal structure of **12** (see below), is that, in **12**, due to hydrogen-bonding interactions between the chlorido ligand and the two ethylenediamine chelates, rapid inversion of the CH_2 groups is slowed down to produce nonaveraged CH_2 groups within each en ring.

Complex **12** is remarkably robust in aqueous solution. Addition of DNO_3 (pD 3.7) causes partial decomposition only within days (with reappearance of resonances due to species **X**), and warming of an aqueous solution of **12** to 40–50 °C for 2 days leads to only gradual and partial formation of AgCl and formation of **X** and other unidentified minor products. From the chemical shifts of the latter, it is evident that they do not contain 1-MeC-*N3* ligands.

X-ray crystal structure of 11 and 12: Crystals of two decomposition products of **10** were isolated from solution after addition of two and four equivalents of NaCl per molecule of **10**, respectively. Figures 7 and 8 give views of the cations of $[Pt_2Pd_2Ag(1\text{-}MeC^-\text{-}N3,N4)_2(NH_2)_2(OH)(NH_3)_2(en)_2](NO_3)_4 \cdot 7\,H_2O$ (**11**) and $[Pt_2Pd_2AgCl(1\text{-}MeC^-\text{-}N3,N4)_2(NH_2)_2(OH)(NH_3)_2(en)_2](NO_3)_3 \cdot 4.5\,H_2O$ (**12**), respectively, and Table 3 lists selected interatomic distances and angles. As can be seen from a comparison of **11** and **12**, the cations are similar as far as their overall appearance is concerned. As compared to **10**, the Ag^+ ions bonded to the O2 sites of

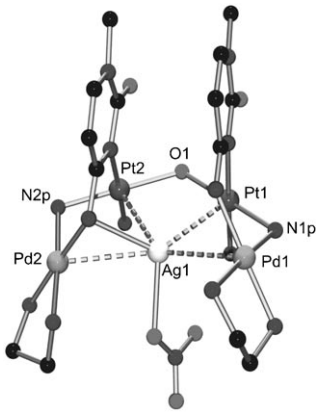

Figure 7. View of cation **11**, obtained from **10** upon removal of the Ag2 and Ag2′ ions by addition of NaCl (2 equiv per molecule of **10**).

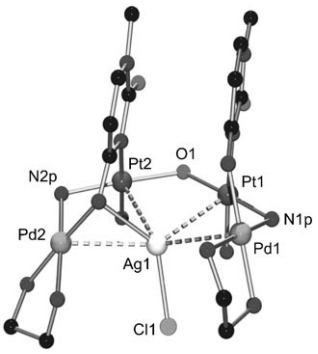

Figure 8. View of cation **12**, obtained from **10** upon addition of an excess of NaCl.

Table 3. Crystallographic data and structure refinement of **10**, **11**, and **12**.

	10	**11**	**12**
formula	$Pt_2Pd_2Ag_2$ $C_{14}H_{47}N_{19}O_{22}$	Pt_2Pd_2Ag $C_{14}H_{53}N_{18}O_{22}$	Pt_2Pd_2AgCl $C_{14}H_{39}N_{17}O_{16.5}$
formula weight [g mmol^{-1}]	1652.43	1536.59	1455.92
crystal system	monoclinic	triclinic	monoclinic
space group	*C*2/*c*	$P\bar{1}$	*C*2/*c*
a [Å]	22.681(5)	10.527(2)	32.586(7)
b [Å]	15.522(3)	14.227(3)	10.235(2)
c [Å]	25.784(5)	16.263(3)	27.278(6)
α [°]	90	113.34(3)	90
β [Å]	110.78(3)	101.18(3)	117.49(3)
γ [Å]	90	96.45(3)	90
Z	8	2	8
V [Å^3]	8487(3)	2145.0(7)	8071(3)
ρ_{calcd} [g cm^{-1}]	2.587	2.379	2.396
μ ($Mo_{K\alpha}$) [mm^{-1}]	8.401	7.864	8.407
F(000)	6256	1468	5488
reflns collected	9734	9833	8783
reflns observed ($I>2\sigma(I)$)	5716	4494	3435
parameters refined	551	527	462
R_1	0.0385	0.0480	0.0442
wR_2	0.1024	0.1011	0.0879
GOF	0.962	0.813	0.771
residual ρ_{max}, ρ_{min} [e Å^{-3}]	2.775, −1.212	2.149, −2.303	0.943, −0.691

the 1-MeC$^-$ ligands are absent. The major difference between **10** on one hand and **11** and **12** on the other is the changes that have occurred in the coordination sphere of the Ag1 atom (Figure 9). These involve the intermetallic

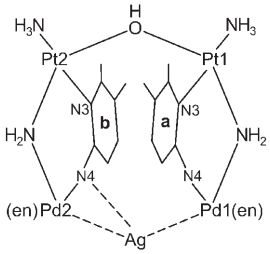

Figure 9. Simplified view of the unsymmetrical interaction of the Ag^+ ion with the N4 sites of (1-MeC$^-$) ligands a and b in **11** and **12**.

Ag1–Pt/Pd and Ag1–N4(1-MeC$^-$) distances (see Table 2). Thus, the Ag1–Pd1 distances increase markedly in **11** (by approximately 0.28 Å) and in **12** (by approximately 0.12 Å), and the asymmetry in the bonding interactions between the Ag1 atom and the N4 sites of 1-MeC$^-$ bases a and b that was seen in **10** (2.743(8) versus 2.388(8) Å) is reserved in **11** and **12**, with the differences being considerably larger. In fact, in **12** the Ag1–N4a separation is too long to be regarded as a bonding interaction. However, this asymmetry appears to be a solid-state effect, as it does not translate into nonequivalent 1-MeC$^-$ ligands in solution, at least not on the ^{1}H NMR timescale. In the ^{1}H NMR spectrum, only single sets of 1-MeC$^-$ resonances are observed for **11** and **12**.

Packing diagrams of **11** and **12** are given in the Supporting Information. Certainly the most remarkable feature of **12** is the presence of an isolated Ag^+Cl^- ion pair ("molecular AgCl") in the solid-state structure and the surprising relative inertness in aqueous solution (see above). There exist a fair number of X-ray structurally characterized examples of chloroargentates(I), as well as heteronuclear Pt,Ag complexes with chlorido bridges. Ag–Cl distances in these compounds are rather variable and depend both on the coordination number of the Ag^+ ion and crystal packing forces, among other factors. For example, in the linear $AgCl_2^-$ ion, Ag–Cl bonds are as short as 2.328(2) and 2.330(2) Å,[23] which is reasonably close to the 2.281 Å separation found in the gas-phase AgCl monomer.[24] In $[Ag_2Cl_4]^{2-}$, which contains trigonal-planar Ag^+ ions, Ag–Cl distances range from 2.359(2) to 2.809(2) Å,[25] and in a dinuclear mixed N,P-ligand complex with Ag(μ-Cl)Ag bridges and tetrahedral Ag^+ coordination geometries, these distances are between 2.601(9) and 2.701(4) Å,[26] very much as in an $Ag_4(\mu_3$-Cl) cluster.[27] Typical Ag–Cl bond lengths in mixed Pt(μ-Cl)Ag complexes, as described by Usón, Forniés, and co-workers, are in the order of 2.41(1)–2.56(1) Å.[18,28] The Ag–Cl bond distance in compound **12** (2.459(3) Å) is in the range of those in the latter compounds, even though the chlorido ligand is terminal, rather than bridging.

Conclusions

The present study on the simultaneous interaction of a single nucleobase (1-methylcytosine) with three different metal ions (Pt^{II}, Pd^{II}, Ag^+) provides a wealth of unexpected and, in part, unprecedented features in metal–nucleobase chemistry. First, it is demonstrated that the NH_3 ligands of the antitumor agent cisplatin are anything but inert, as is frequently assumed. In fact, an ammonia ligand can be readily deprotonated, even at pH 6–7, in the presence of other metal ions, to become a bridging amido ligand. Second, the simple pyrimidine nucleobase 1-methylcytosine can act as a tetradentate ligand and can do so by binding three different metal ions. Third, the X-ray crystal structures of **10**, **11**, and **12** reveal an (nb)Pt(OH)Pt(nb) motif (nb: nucleobase) with two parallel, stacked nucleobases in head–head orientations; this corroborates previous proposals on the feasibity of such types of intrastrand DNA cross-links of dinuclear *cis*-$[(NH_3)_2Pt(OH)Pt(NH_3)_2]^{3+}$ species with nucleobases. Fourth, in compound **12**, a rare case of an isolated Ag^+Cl^- ion pair ("AgCl molecule") is realized and is found to be remarkably stable in aqueous solution before it forms a precipitate of AgCl.

Experimental Section

Materials and methods: *cis*-$[PtCl_2(NH_3)_2]$,[29] $[PdCl_2(en)]$,[30] 1-methylcytosine (1-MeC),[31] and *cis*-$[PtCl(NH_3)_2(1\text{-MeC-}N3)]Cl\cdot H_2O$ (**5**),[2d] were prepared as described in the literature. Pyridine (py), pyrazole (Hpz), dimethylformamide (DMF), CH_2Cl_2, 2-aminopyridine (Hampy), K_2PtCl_4, and K_2PdCl_4 were of commercial origin.

***cis*-[Pt(NH$_3$)$_2$(py)(Hpz)](ClO$_4$)$_2$ (1)**: *cis*-$[PtCl_2(NH_3)_2]$ (300 mg, 1 mmol) and $AgNO_3$ (169 mg, 1 mmol) were stirred in DMF (50 mL) for 24 h at 60 °C with daylight excluded. After filtration of AgCl, py (0.95 mmol) was added dropwise. After the reaction mixture had been heated for 1 d at 45 °C and subsequently cooled to room temperature, CH_2Cl_2 (30 mL) was added. The resulting pale-yellow precipitate (207 mg, 51 % yield) was analyzed as $[PtCl(NH_3)_2(py)]NO_3$ (by elemental analysis), but the ^{1}H NMR spectrum reveals the presence of a small amount (< 5 %) of *cis*-$[Pt(NH_3)_2(py)_2]^{2+}$. The identity of the byproduct was confirmed by preparing it through the reaction of *cis*-$[Pt(NH_3)_2(H_2O)_2]^{2+}$ with py (2 equiv). The H2/H6 doublets of the py ligands in $[PtCl(NH_3)_2(py)]NO_3$ in D_2O (pD 6.2; 200 MHz) occur at $\delta = 8.69$ ppm and display characteristic $^3J(^{195}Pt\text{–}^1H)$ satellites of 38 Hz. Other resonances in the ^{1}H NMR spectrum: $\delta = 7.97$ (t, H4), 7.52 (t, H3/H5); in the ^{195}Pt NMR spectrum: $\delta = -2307$ ppm. Attempts to remove the bis(pyridine) complex by recrystallization was unsuccessful. Subsequently, the impure starting material (325 mg, approximately 0.8 mmol) was treated with $AgNO_3$ (135 mg, 0.8 mmol, 30 mL H_2O, 50 °C, 24 h). After filtration of AgCl, pyrazole (53 mg, 1.2 mmol) was added and the mixture stirred at 50 °C for another 24 h. Addition of excess solid $NaClO_4$ (aq) and subsequent cooling of the solution to 4 °C gave **1** as colorless crystals. Yield: 248 mg (54 %); ^{1}H NMR (D_2O, pD 7.2): $\delta = 7.89$ (H3/H5 Hpz), 6.49 (H4 Hpz), 8.64 (H2/H6 py), 7.97 (H4 py), 7.50 ppm (H3/H5 py); ^{195}Pt NMR (D_2O, pD 7.2): $\delta = -2474$ ppm; elemental analysis: calcd (%) for $C_8H_{15}N_5O_8PtCl_2$ (574.2): C 16.7, H 2.6, N 12.2; found: C 16.8, H 2.5, N 12.2.

The pK_a value of the Hpz ligand in **1** was determined by pD-dependent ^{1}H NMR spectroscopy[32] and was found to be 8.13 (D_2O), which corresponds to 7.57 in H_2O.[33]

***cis*-[Pt(NH$_3$)$_2$(py)(Hampy)](ClO$_4$)$_2$·3H$_2$O (2)**: Compound **2** was prepared in analogy to **1** in 68 % yield. ^{1}H NMR (D_2O, 2D-COSY): $\delta = 8.72$ ($^3J(^{195}Pt\text{–}^1H) = 41$ Hz; H2/H6 py), 8.20 ($^3J(^{195}Pt\text{–}^1H) = 37$ Hz; H6 Hampy), 7.95 (H4 py), 7.50 (H4 Hampy, H3/H5 py), 6.66 ppm (H3/H5 Hampy); elemental analysis: calcd (%) for $C_{10}H_{23}N_5O_6PtCl_2$ (655.3): C 18.3, H 3.5, N 10.7; found: C 18.4, H 3.0, N 10.7.

[Pt(μ-pz)(μ-NH$_2$)(NH$_3$)(py)Pd(en)](ClO$_4$)$_2$ (3): A solution of **1** (115 mg, 0.2 mmol) in water (15 mL) was combined with an aqueous solution of $[Pd(en)(H_2O)_2](NO_3)_2$ (0.2 mmol in H_2O (5 mL), prepared from $[PdCl_2(en)]$ and $AgNO_3$ (2 equiv) with filtration of AgCl) and the pH value of the solution was adjusted to approximately 8.5 by means of 1 N NaOH. After the mixture had been stirred for 24 h (pH 7.2 at end), solid $NaClO_4$ (aq) was added, and the sample was cooled to 4 °C. Within 5 h, a pale-yellow precipitate of **3** had formed. The yield was 79.9 mg (54 %). ^{1}H NMR (D_2O, pD 7.2): $\delta = 8.77$ (d, $J = 6.4$ Hz, $^3J(^{195}Pt\text{–}^1H) = 39$ Hz; H2/H6 py), 8.05 (t; H4, py), 7.60 (m; H3/H5 py), 7.23 (H5 pz), 6.55 (H3 pz), 6.07 (H4 pz), 2.82 (CH_2 en), 1.53 ppm ($^2J(^{195}Pt\text{–}^1H) = 46$ Hz; μ-NH_2); ^{195}Pt coupling constants for the pz resonances (H5, 10 Hz; H3, 11 Hz; H4, 9 Hz) are observed in the ^{195}Pt-edited ^{1}H NMR spectrum only (see the Supporting Information, Figure S1); elemental analysis: calcd (%) for $C_{10}H_{21}N_7O_8Cl_2PdPt$ (739.7): C 16.2, H 2.9, N 13.3; found: C 16.1, H 2.9, N 13.4.

[Pt(μ-ampy)(μ-NH$_2$)(NH$_3$)(py)Pd(en)](NO$_3$)$_2$ (4): Compound **4** was isolated in a semipreparative way analogous to that for **3** by starting from **2** and $[Pd(en)(H_2O)_2](NO_3)_2$, yet at a higher initial pH value (pH 10, dropped to pH 5.5 within 24 h at room temperature) and without extra $NaClO_4$ added. ^{1}H NMR (D_2O, 2D-COSY): $\delta = 8.70$ (H2/H6 py), 7.98 (H4 py), 7.48 (H3/H5 py, H6 Hampy), 7.15 (H4 Hampy), 6.69 (H3 ampy), 6.12 (H5 ampy), 1.60 ppm (μ-NH_2).

[{Pt$_2$(1-MeC$^-$-*N3*,*N4*)$_2$(NH$_3$)$_2$(NH$_2$)$_2$(OH)Pd$_2$(en)$_2$Ag}$_2${Ag(H$_2$O)}$_2$](NO$_3$)$_{10}$·6H$_2$O (10): *cis*-$[Pt(NH_3)_2(1\text{-MeC-}N3)(H_2O)](NO_3)_2$ and $[Pd(en)(H_2O)_2](NO_3)_2$ were prepared by treating **5** (561 mg, 1.27 mmol in H_2O (7 mL)) and $[PdCl_2(en)]$ (322 mg, 1.36 mmol in H_2O (7 mL)) with $AgNO_3$ (2 equiv each) separately in the dark (room temperature, 1 d or longer). After filtration of AgCl, the two solutions were combined and the pH value was raised to 5.6 by adding NaOH (approximately 2 equiv). Subsequently, solid $AgNO_3$ (250 mg, 1.48 mmol) was added. At this stage, the solution was filtered to remove a small amount of precipitate and the pH value (now 4.5) was re-adjusted to 5.3 by addition of NaOH. Slow evaporation of the yellow solution under a flow of N_2 gave **10** as yellow cubes. The yield was 294 mg (28 % based on Pt). ^{1}H NMR: see Table 1; elemental analysis: calcd (%) for $C_{28}H_{94}N_{38}O_{44}Pt_4Pd_4Ag_4$ (3304.9): C 10.2, H 2.9, N 16.1; found: C 10.3, H 2.7, N 16.4.

[Pt$_2$Pd$_2$Ag(1-MeC$^-$-*N3*,*N4*)$_2$(NH$_2$)$_2$(OH)(NH$_3$)$_2$(en)$_2$](NO$_3$)$_4$·7H$_2$O (11): NaCl (1.98 equiv, 1.5 mg, 0.025 mmol) was added to a solution of **10** in water (41.6 mg in 15 mL, 0.0126 mmol). The mixture was stirred for 1 h in the dark. A yellow solution was obtained after centrifugation of AgCl. After slow evaporation (3 d) at 5 °C, yellow crystals were harvested and characterized by X-ray crystallography and ^{1}H NMR (see Table 1). According to ^{1}H NMR spectroscopy, **10** reacts quantitatively to form **11**. To avoid contamination with formed $NaNO_3$, no attempt was made to optimize the isolated yield.

[Pt$_2$Pd$_2$AgCl(1-MeC$^-$-*N3*,*N4*)$_2$(NH$_2$)$_2$(OH)(NH$_3$)$_2$(en)$_2$](NO$_3$)$_3$·4.5H$_2$O (12): A similar procedure to that used for **11** was carried out. In this case, NaCl (4.07 equiv, 2.8 mg, 0.048 mmol) was added to **10** (39.1 mg, 0.0118 mmol) dissolved in water (10 mL). After the mixture had been stirred for 30 min in the dark, AgCl was centrifuged off. The resulting pale-yellow solution was kept for 1 d at room temperature. Pale-yellow needles of **12** had then formed, which were characterized by X-ray crystallography and ^{1}H NMR (see Table 1). According to a ^{1}H NMR spectroscopic experiment, **12** is formed quantitatively. The yield of isolated product was not determined to avoid contamination with $NaNO_3$.

Characterization and NMR measurements: Elemental (C, H, N) analysis data were obtained on a Leco CHNS-932 instrument. ^{1}H NMR spectra in D_2O were recorded on Varian Mercury 200 FT NMR and Bruker DRX 400 instruments with sodium-3-(trimethylsilyl)propanesulfonate (TSP, $\delta = 0$ ppm) as the internal reference. ^{195}Pt NMR spectra were recorded on a Bruker AC 200 (42.998 MHz) spectrometer at 20 °C and referenced against external Na_2PtCl_6 ($\delta = 0.0$ ppm). ^{195}Pt satellites in the spectrum of **3** were identified by means of the ^{1}H–^{195}Pt editing tech-

nique[34] by using standard programmes. Application of this technique suppresses those ^{1}H NMR signals that do not couple with the ^{195}Pt nucleus. pD values of NMR samples were determined by use of a glass electrode and addition of 0.4 units to the uncorrected pH meter reading (pH*). For the determination of the pK_a value of **1**, samples were dissolved in D_2O and the pD value was adjusted by addition of NaOD.

X-ray crystallography: Data collection was performed on an Enraf–Nonius Kappa CCDC diffractometer by using graphite-monochromated $Mo_{K\alpha}$ radiation ($\lambda = 0.71069$ Å).[35] Data reduction and cell refinement were carried out by using the programs DENZO and SCALEPACK.[36] The intensities of the reflections were collected at room temperature. All of the structures were solved by standard Patterson methods[37] and refined by full-matrix least-squares methods based on F^2 by using WINGX[38] software. All non-hydrogen atoms in the structures were refined anisotropically, except several nitrate counteranions and several water molecules. The hydrogen atoms were placed in geometrically idealized positions (except those of water molecules) according to geometrical considerations and refined with isotropic displacement parameters according to the riding model. Crystal data, details of data collection, and refinement parameters for compounds **10**, **11**, and **12** are summarized in Table 1.

CCDC-665285, 665286, and 665287 contain the supplementary crystallographic data for this paper. These data can be obtained free of charge from The Cambridge Crystallographic Data Centre via www.ccdc.cam.ac.uk/data_request/cif.

Acknowledgements

Financial support by the Deutsche Forschungsgemeinschaft (DFG) and the Fonds der Chemischen Industrie (FCI) is gratefully acknowledged. We thank COST D39 for an STSM for P.J.S.M.

[1] See, for example, various articles in *Cisplatin—Chemistry and Biochemistry of a Leading Anticancer Drug* (Ed.: B. Lippert), Helvetica Chimica Acta and Wiley-VCH, Zürich and Weinheim, **1999**.
[2] See, for example: a) I. A. G. Roos, A. J. Thomson, J. Eagles, *Chem.-Biol. Interact.* **1974**, *8*, 421; b) B. Lippert, C. J. L. Lock, R. A. Speranzini, *Inorg. Chem.* **1981**, *20*, 808; c) R. Beyerle, B. Lippert, *Inorg. Chim. Acta* **1982**, *66*, 141; d) T. Wienkötter, M. Sabat, G. Fusch, B. Lippert, *Inorg. Chem.* **1995**, *34*, 1022; e) J. K.-C. Lau, D. Deubel, *Chem. Eur. J.* **2005**, *11*, 2849.
[3] a) A. Schneider, E. Freisinger, B. Beck, B. Lippert, *J. Chem. Soc. Dalton Trans.* **2000**, 837; b) B. Beck, A. Schneider, E. Freisinger, D. Holthenrich, A. Erxleben, A. Albinati, E. Zangrando, L. Randaccio, B. Lippert, *Dalton Trans.* **2003**, 2533.
[4] a) S. Park, A. L. Rheingold, D. M. Roundhill, *Organometallics* **1991**, *10*, 615; b) J. Ruiz, M. T. Martínez, C. Vicente, G. García, G. López, P. A. Chaloner, P. B. Hitchcock, *Organometallics* **1993**, *12*, 4321; c) M. S. Driver, J. F. Hartwig, *Organometallics* **1997**, *16*, 5706; d) M. S. Driver, J. F. Hartwig, *J. Am. Chem. Soc.* **1996**, *118*, 4206; e) J. J. Li, W. Li, A. J. James, T. Holbert, T. P. Sharp, P. R. Sharp, *Inorg. Chem.* **1999**, *38*, 1563; f) U. Anandhi, T. Holbert, D. Lueng, P. R. Sharp, *Inorg. Chem.* **2003**, *42*, 1282.
[5] a) M. Kretschmer, L. Heck, *Z. Anorg. Allg. Chem.* **1982**, *490*, 215; b) L. Heck, M. Ardon, A. Bino, J. Zapp, *J. Am. Chem. Soc.* **1988**, *110*, 2691; c) W. Frank, L. Heck, S. Müller-Becker, T. Raber, *Inorg. Chim. Acta* **1997**, *265*, 17.
[6] W. Saenger, *Principles of Nucleic Acid Structure*, Springer, New York, **1984**, p. 53.
[7] G. Yagil, *Tetrahedron* **1967**, *23*, 2855.
[8] J. F. Britten, B. Lippert, C. J. L. Lock, P. Pilon, *Inorg. Chem.* **1982**, *21*, 1936.
[9] F. Schwarz, B. Lippert, A. Iakovidis, N. Hadjiliadis, *Inorg. Chim. Acta* **1990**, *168*, 275.
[10] R. Faggiani, B. Lippert, C. J. L. Lock, R. A. Speranzini, *J. Am. Chem. Soc.* **1981**, *103*, 1111.
[11] B. Lippert, C. J. L. Lock, R. A. Speranzini, *Inorg. Chem.* **1981**, *20*, 335.
[12] a) F. D. Rochon, A. Morneau, R. Melanson, *Inorg. Chem.* **1988**, *27*, 10; b) F. D. Rochon, R. Melanson, *Acta Crystallogr. Sect. C* **1988**, *44*, 474.
[13] B. M. Still, P. G. A. Kumar, J. R. Aldrich-Wright, W. S. Price, *Chem. Soc. Rev.* **2007**, *36*, 665.
[14] D. Holthenrich, E. Zangrando, E. Chiarparin, B. Lippert, L. Randaccio, *J. Chem. Soc. Dalton Trans.* **1997**, 4407.
[15] D. Holthenrich, M. Krumm, E. Zangrando, F. Pichierri, L. Randaccio, B. Lippert, *J. Chem. Soc. Dalton Trans.* **1995**, 3275.
[16] These distances are longer than those within the Ag^+-bridged pairs of neutral 1-MeC in $[Ag(1\text{-MeC-}N3,O2)NO_3]_2$, in which Ag–O2 bonds of 2.367(2) Å are observed: T. J. Kistenmacher, M. Rossi, L. G. Marzilli, *Inorg. Chem.* **1979**, *18*, 240.
[17] T. Yamaguchi, F. Yamazaki, T. Ito, *J. Am. Chem. Soc.* **2001**, *123*, 743.
[18] R. Usón, J. Forniés, *Inorg. Chim. Acta* **1992**, *198–200*, 165, and references cited therein.
[19] See, for example: a) H. Schöllhorn, U. Thewalt, B. Lippert, *J. Chem. Soc. Chem. Commun.* **1984**, 769; b) B. Lippert, H. Schöllhorn, U. Thewalt, *Inorg. Chem.* **1987**, *26*, 1736.
[20] See, for example: a) J. Ruiz, V. Rodríguez, G. López, P. A. Chaloner, P. B. Hitchcock, *J. Chem. Soc. Dalton Trans.* **1997**, 4271; b) C. Tejel, M. A. Ciriano, M. Bordonaba, J. A. López, F. J. Lahoz, L. A. Oro, *Inorg. Chem.* **2002**, *41*, 2348; c) S. Kannan, A. J. James, P. R. Sharp, *Inorg. Chim. Acta* **2003**, 345, 8.
[21] B. Spingler, M. Scavany-Grigorieff, A. Werner, H. Berke, S. J. Lippard, *Inorg. Chem.* **2001**, *40*, 1065.
[22] A. P. Hitchcock, C. J. L. Lock, W. M. C. Pratt, B. Lippert in *Platinum, Gold, and Other Metal Chemotherapeutic Agents, ACS Symposium Series 209* (Ed.: S. J. Lippard), American Chemical Society, Washington, D.C., **1983**, pp. 209–227.
[23] G. Helgesson, S. Jagner, *Inorg. Chem.* **1991**, *30*, 2574.
[24] L. C. Krisher, W. G. Norris, *J. Chem. Phys.* **1966**, *44*, 391.
[25] G. Helgesson, S. Jagner, *J. Chem. Soc. Dalton Trans.* **1990**, 2413.
[26] N. W. Alcock, P. Moore, P. A. Lampe, K. F. Motz, *J. Chem. Soc. Dalton Trans.* **1982**, 207.
[27] C. W. Liu, B.-J. Liaw, L.-S. Liou, J.-C. Wang, *Chem. Commun.* **2005**, 1983.
[28] a) R. Usón, J. Forniés, M. Tomás, I. Ara, J. M. Casas, *Polyhedron* **1992**, *11*, 1783; b) R. Usón, J. Forniés, M. Tomás, J. M. Casas, F. A. Colton, L. R. Falvello, *Inorg. Chem.* **1986**, *25*, 4519; c) R. Usón, J. Forniés, M. Tomás, I. Ara, *Inorg. Chem.* **1994**, *33*, 4023.
[29] a) S. C. Dhara, *Indian J. Chem.***1970**, *8*, 193; b) G. Raudaschl-Sieber, B. Lippert, J. D. Hoeschele, H. E. Howard-Lock, C. J. L. Lock, P. Pilon, *Inorg. Chim. Acta* **1985**, *106*, 141.
[30] B. J. McCormick, E. N. Jaynes, Jr., R. I. Kaplan, *Inorg. Synth.* **1972**, *13*, 216.
[31] T. J. Kistenmacher, M. Rossi, J. P. Caradonna, L. G. Marzilli, *Adv. Mol. Relax. Interact. Proc.* **1979**, *15*, 119.
[32] R. Tribolet, H. Sigel, *Eur. J. Biochem.* **1987**, *163*, 353.
[33] R. B. Martin, *Science* **1963**, *139*, 1198.
[34] A. Bax, R. H. Griffey, B. L. Hawkins, *J. Magn. Reson.* **1983**, *55*, 301.
[35] KappaCCD package, Nonius, Delft, The Netherlands, **1997**.
[36] DENZO and SCALEPACK: Z. Otwinowsky, W. Minor, *Methods Enzymol.* **1997**, *276*, 307.
[37] G. M. Sheldrick, *Acta Crystallogr. Sect. A* **1990**, *46*, 467.
[38] L. J. Farrugia, *J. Appl. Crystallogr.* **1999**, *32*, 837.

Received: March 31, 2008
Published online: June 23, 2008

